Nat Hazards (2016) 80:367–388
DOI 10.1007/s11069-015-1972-7

ORIGINAL PAPER

Spatial analysis of meteorological drought return periods in China using Copulas

Xiong-Fei Liu[1,2] · Shi-Xin Wang[1] · Yi Zhou[1] · Fu-Tao Wang[1] · Guang Yang[1] · Wen-Liang Liu[1]

Received: 21 April 2015 / Accepted: 16 September 2015 / Published online: 14 October 2015

Abstract China is considered to be one of the most vulnerable drought-prone countries in the world, and it has recently suffered many severe droughts with large economic and societal losses. Drought events in China have been extracted using run theory based on the Standardized Precipitation Evapotranspiration Index, which covers the period 1961–2013 across 810 stations. The drought events are characterized by three variables: duration, severity and peak. Exponential, Weibull and Pareto functions are then selected to describe the marginal distribution of duration, severity and peak, respectively. The Gumbel–Hougaard Copula was used to construct the joint distribution of Duration–Severity and Duration–Peak, while the Clayton Copula and the Gaussian Copula are used to construct the joint distribution of Severity–Peak and Duration–Severity–Peak, respectively. The results indicate that the return period is dependent on spatial location, variable type and the combination of variables. For extreme droughts, trivariate 'and' return periods are longer, with an average of 42.1 years. The short return period is mainly distributed in southern China, especially on the border between Sichuan and Yunnan, the coastal regions of Guangdong, western Hunan and northern Jiangxi. Studies on the identification of spatial distributions of drought return periods across China have therefore been undertaken for drought mitigation and strategy planning.

Keywords Return period · Drought · Copulas · Standardized Precipitation Evapotranspiration Index · China

✉ Yi Zhou
zhouyi@radi.ac.cn

1 State Key Lab of Remote Sensing Science, Institute of Remote Sensing and Digital Earth, Chinese Academy of Sciences, Beijing 100101, People's Republic of China

2 University of Chinese Academy of Sciences, Beijing 100049, People's Republic of China

1 Introduction

Drought is an insidious natural hazard that results from a deficiency of water availability, compared to what is expected or normal. This departure from normality can result in insufficient water supply to meet the demands of human activities, the environment and can cause serious agricultural, environmental and socioeconomic damage. Drought ranks first among all natural hazards in terms of the number of people affected for its long duration, wide areal extent and severe negative socioeconomic impacts (Mishra and Singh 2010). It is the world's costliest natural hazard, causing an average \$6–\$8 billion in global damages annually (Wilhite 2000). In recent years, droughts have occurred more frequently, with their impacts aggravated by the rise in water demand and the variability in water resources due to the extreme weather (Lu et al. 2011; Wang et al. 2014). Droughts may occur in humid as well as in arid regions, but the characteristics differ significantly from one region to another. Drought events are customarily characterized by onset, termination, duration, severity, peak and total areal extent (Wilhite and Glantz 1985). Understanding the spatiotemporal variations of drought across different scales presents a significant challenge. Numerous studies have consequently been conducted for drought prevention and management (Andreadis and Lettenmaier 2006; Gocic and Trajkovic 2014; Mishra and Desai 2005; Vicente-Serrano 2006).

Return periods have been widely used to quantify drought risk, and it can improve high-level drought hazard mitigation, strategy planning and program design. A typical example is the estimation of drought conditions for the design of water resource facilities. As droughts are complex, stochastic processes with multi-attributes in nature, accurate methods to explore drought characteristics are through probabilistic theory and stochastic process methods. Yevjevich first introduced the concept of run theory to analyze droughts (Yevjevich and Ingenieur 1967), which was later supported by a significant amount of researches by others (Janga Reddy and Ganguli 2012). Before 2006, drought frequency and return period analysis were mainly based on univariate statistical analysis by calculating the frequency of drought duration, severity, peak and area (Bonaccorso et al. 2003; Kim et al. 2003). Similarly, few researchers have attempted to analyze the multivariate characteristics of drought events to get joint return periods (González and Valdés 2003; Kim et al. 2006). To calculate the joint distribution function, drought variables are usually treated as uncorrelated, or are expected to follow the same marginal distribution. As there is a certain degree of correlation between variables, which describe the same drought event, these hypotheses may not always be in accordance with reality.

Copulas make it possible to model the probabilistic dependence structure, independently of marginal distribution. Its major advantage is allowing multi-variables to be described using different marginal distributions. Copula was initially introduced in insurance and finance context to explore abnormally high risks, and was then developed for use in hydrological research to analyze flood risks (da Costa Dias 2004; Favre et al. 2004). Since Shiau (2006) first introduced Copulas to drought return period analysis, many researchers have used this methodology to study drought frequency and return period. For example, Serinaldi et al. (2009) applied Student Copula to the probabilistic analysis of drought characteristics in Sicily and calculated the return period of critical drought events. Similarly, Shiau et al. employed the Clayton Copula to model the correlation between drought duration and severity in Iran, and found the difference in the return period between Abadan and Anzali (Shiau and Modarres 2009). Liu et al. (2011) used the Archimedean Copula to determine the spatial distribution of drought joint probability in Guangdong, China, and found that the probability of a drought occurring in southern Guangdong was higher than that in the north. Mirabbasi et al. (2012) found that the Galambos Copula provided the best fitness for the observed drought data at the Sharafkhaneh Station in Iran. Xiao et al. (2012) studied Archimedean Copulas, including the Gumbel–Hougaard, Clayton and Frank Copula, to determine the spatial analysis of drought in the Pearl River Basin of China. This research concluded that the Gumbel–Hougaard Copula was suitable to use for most sites. These researchers mainly studied Copulas characteristics and employed Copula to construct the joint distribution in a few sites or across small areas (Liu et al. 2011; Michele et al. 2013; Zhang et al. 2012, 2015). However, as droughts generally cover large areas, drought return periods in small areas cannot provide effective support for drought management at a national level. Therefore, it is urgently required to select the best marginal distribution function and the best Copula function for large areas, and product the spatial distribution of drought return periods.

China is a vast country with a diverse climate, including humid, semi-humid, semiarid and arid climatic zones. Variations in precipitation and temperature, both spatially and over time, lead to China being especially prone to drought-related hazards. For example, a large-scale drought disaster occurred in Yunnan Province from November 2009 to March 2010, and threatened 9.65 million residents with a shortage of drinking water (Lu et al. 2012). From January through to May 2011, the middle and lower reaches of Yangtze River were plagued by the drought, affecting approximately 37,970 km^2 of arable land (State Flood Control and Drought Relief Office and the Ministry of Water Resources of the People's Republic of China 2011). These recent drought events were accompanied by a decrease in precipitation and abnormal high temperature. In order to identify droughts that occurred as a result of higher temperature, Standardized Precipitation Evapotranspiration Index (SPEI) was used to consider the influence of temperature. Researches undertaken to assess drought using the SPEI have shown it to be particularly effective in detecting drought conditions (Hernandez and Uddameri 2014; Lorenzo-Lacruz et al. 2010). However, no research has been undertaken to study the drought return periods based on SPEI.

This work will address the spatial distribution of drought return period across China using SPEI and Copula. The main objectives of this study are: (1) to provide the spatial distribution of best marginal distribution for three drought characteristics; (2) to provide the spatial distribution of the best Copula function for bivariate and trivariate joint distribution; and (3) to analyze the spatial distribution of drought return period of specific scenarios.

2 Study area and data

Eastern China is dominated by the East Asian Summer Monsoon. Southwest China is dominated by a combination of the East Asian Summer Monsoon and the Indian Summer Monsoon, while Northwest China remains unaffected by the Monsoons. Over the past 50 years, average annual precipitation has shown a gradual variation, from 15 mm to over 2000 mm from the northwest to the southeast. Annual mean temperatures also show variation from the north to the south of the country, with a range of -12 to 25 °C. The spatial distribution of annual precipitation and annual temperature in China is shown in Fig. 1. The precipitation and temperature are uneven in spatial and temporal, leading to the frequent occurrence of droughts in China. The average area influenced by drought is approximately 216,000 km^2 per year, which results in a 161.18×10^8 kg grain loss

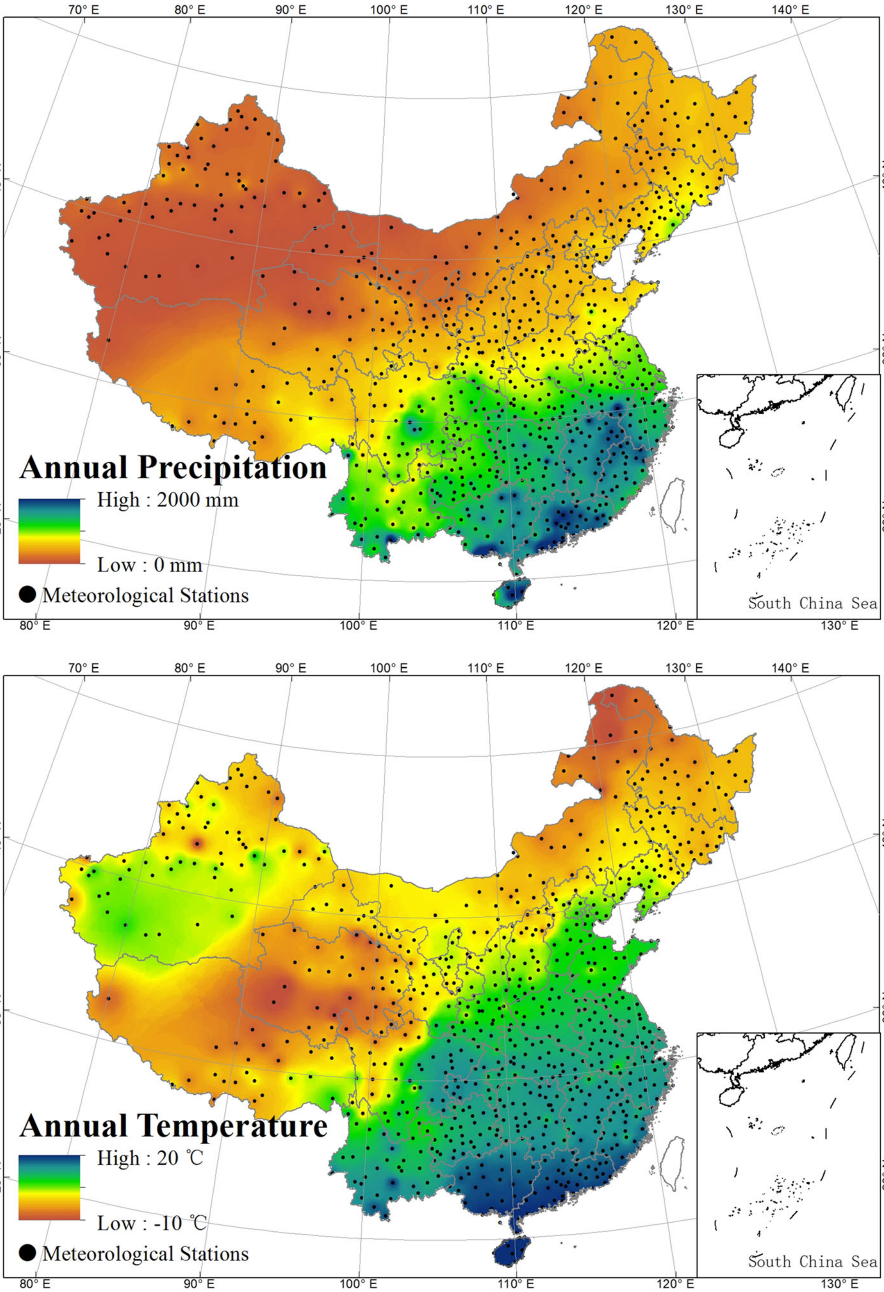

Fig. 1 Annual precipitation and temperature in China

(Qiu et al. 2013). Generally, the direct economic loss in a dry year accounts for 1.1 % of the gross domestic product (GDP), while in a severe drought year, this may increase to a loss of 2.5–3.5 % of the GDP (Zhang 2009).

The China surface climate daily dataset (V3.0) and China surface climate monthly dataset (V3.0) were downloaded from China Meteorological Data Sharing Service System (http://cdc.nmic.cn/home.do). Data quality has already been checked by the China Meteorological Administration. These two datasets were combined to a new monthly dataset with less missing data. The data records covering the period from 1961 to 2013 were used, owing to most stations have not been built before 1961. Twenty-nine stations with missing data longer than 120 months were removed. This would guarantee that the data length of 810 selected stations is longer than or equal to 43 years. Ordinary Kriging method was utilized to interpolate the remnant few missing data (Atkinson and Lloyd 1998). Taiwan Province is not included in this study for the necessary data were not available. Locations of meteorological stations are also shown in Fig. 1. The sites are sparse in the west, especially the western Tibet. The interpolation results may have a large deviation from the actual situation in this place.

3 Methodology

3.1 Standardized Precipitation Evapotranspiration Index

The Standardized Precipitation Evapotranspiration Index (SPEI) was established by Vicente-Serrano (2010a). It effectively describes the water deficit with multiple timescales, reflecting the ability of precipitation and evapotranspiration to influence different water resources. SPEI is also a normalized function, which is capable of eliminating data discrepancies caused by spatiotemporal distributions, and is used to facilitate the comparison. More details of the SPEI can be obtained from previous articles (Vicente-Serrano et al. 2010a, b), and SPEI Web site (http://sac.csic.es/spei/map/maps.html). In this paper, the Thornthwaite (1948) function was used to calculate evapotranspiration. This function has the advantage of only requiring monthly mean temperature and site location. Three-month SPEI, which reflects the seasonal changes, was used to extract the drought events.

Based on SPEI, the drought conditions can be classified into many categories. A negative SPEI value indicates the occurrence of droughts. SPEI value was divided with 0.5 steps in this study. The meteorological condition can be classified into five categories based on SPEI according to Table 1.

3.2 Run theory

Currently, the most commonly used method to identify droughts is the run theory (Yevjevich and Ingenieur 1967). Drought characteristics, including onset, termination, duration, severity and peak, can be recognized easily by this method. Figure 2 shows the definition

Table 1 Categorization of dryness grade by the SPEI

SPEI	Categories
$-0.5 < \text{SPEI}$	Normal or wetness
$-1.0 < \text{SPEI} \leq -0.5$	Slight dryness
$-1.5 < \text{SPEI} \leq -1.0$	Moderate dryness
$-2.0 < \text{SPEI} \leq -1.5$	Severe dryness
$\text{SPEI} \leq -2.0$	Extreme dryness

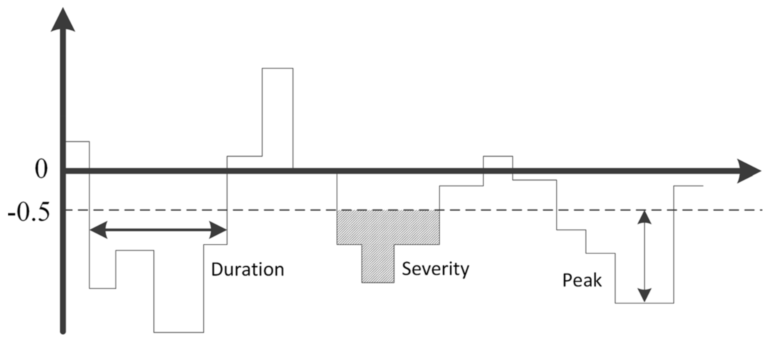

Fig. 2 Definition of drought events using run theory

of drought events and drought variables based on SPEI using run theory. A drought event is defined as a period where the SPEI is less than the truncation value (e.g., -0.5 in this study). An SPEI value less than -0.5 indicates that a drought has occurred, and will be ongoing until the SPEI value is greater than -0.5. The drought duration, D, is the length of drought event; the severity of droughts, S, is calculated by the cumulative SPEI over the course of drought event; and the peak, P, is the minimum recorded SPEI during one drought event. Since the SPEI severity and peak are always negative, absolute values have been assumed for simplicity in the subsequent work.

3.3 Marginal distribution of drought characteristics

Many researchers have studied the marginal distribution of different drought variables (Mirakbari et al. 2010; Song and Singh 2010; Wong et al. 2009). It has been demonstrated that the best marginal distribution varies with the drought index and the variable type. However, the research undertaken shows that no unified conclusion has been reached to data on the marginal distribution of drought characteristics based on SPEI. In this study, four commonly used two-parameter distributions (Gaussian, Exponential, Weibull and Gamma) and two three-parameter distributions (GEV and GDP) were tested as outlined in Table 2. Parameters of these marginal distributions were estimated by the maximum likelihood estimation method (MLE).

Table 2 Cumulative distribution function of six marginal distributions

Function	Cumulative distribution function
Gaussian distribution	$F(x) = \frac{1}{\sqrt{2\pi}}\int_{-\infty}^{x} \exp\left(-\frac{(x-\beta)^2}{2\alpha^2}\right)\mathrm{d}x$
Exponential distribution	$F(x) = 1 - \exp\left(-\frac{x-\beta}{\alpha}\right)$
Weibull distribution	$F(x) = 1 - \exp\left(-\frac{x}{\alpha}\right)^{\beta}$
Gamma distribution	$F(x) = \int_0^x \frac{x^{\alpha-1}}{\beta^{\alpha}\Gamma(\alpha)}\exp\left(-\frac{x}{\beta}\right)\mathrm{d}x$
Generalized Pareto distribution	$F(x) = 1 - \left[1 - \lambda\left(\frac{x-\beta}{\alpha}\right)\right]^{\frac{1}{\lambda}}$
Generalized Extreme Value Distribution	$F(x) = \exp\left\{-\left[1 - \lambda\left(\frac{x-\beta}{\alpha}\right)\right]^{1/\lambda}\right\}$

In order to select the best marginal distribution for all drought characteristics, the Akaike information criterion (AIC) was used to test the fitting result (Akaike 1974). This method was also used to select the best Copula function. AIC encourages improvement of the goodness of fit, and simultaneously avoids the potential to overfit the data. The goodness of fit is improved when the AIC is smaller. The calculation of AIC is shown in Eq. (1).

$$\mathrm{AIC} = 2k + n\ln(\mathrm{MSE}) \tag{1}$$

where k is the number of parameters, n is sample size, and *MSE* is the mean square error.

3.4 Copula

Recently, Copula is developing quickly, and has shown great potential for multivariate joint distribution analysis and multivariate frequency analysis. It can describe the dependence structure between variables and allow for the calculation of joint probabilities, independently of the marginal behavior of the involved variables (Gräler et al. 2013). It can simply combine several univariate marginal distributions into their joint distribution. Copula has flexible forms and can deal with a variety of conditions. The maximum likelihood method is commonly used to estimate the parameters. More details can be found in previous papers (Nelsen 1999; Sklar 1959). Copulas have been widely used in the area of insurance, finance, stock and hydrology to predict the probability of extreme events. For now, most researches focus on the joint distribution of two variables.

Among all Copula families, the Elliptical Copula family and the Archimedean Copula family have been widely used in the area of hydrology and drought. There is a variety of forms for both two Copula families. In this study, the Elliptical Copulas (Normal Copula and t Copula) and the Archimedean Copulas (Clayton Copula, Gumbel–Hougaard Copula and Frank Copula) are selected to analyze the joint probability of drought events for their simplicity and wide representation. More details can be found in previous studies(Joe 1997; Song et al. 2012).

A triplet can be fitted by Elliptical Copulas and Archimedean Copulas. However, it is necessary that the three pairs have the same dependence when using Archimedean Copulas, which is usually difficult (Grimaldi and Serinaldi 2006). To avoid this problem, asymmetric Copula, nested Copula and Vine Copula can be adopted. In order to improve the processing speed, nested Copula was chosen to fit the trivariate joint distribution.

3.5 Return period

The return period can provide effective support for decisions surrounding drought prevention and management. The calculation of drought multivariate return period is based on univariate marginal distribution and multivariate joint distribution. Gräler provided an overview about the multitude of definitions and practical implications of multivariate return period (Gräler et al. 2013).

The univariate return period of drought characteristics, when greater than or equal to the given value, can be calculated by Eq. 2.

$$T = \frac{E}{1 - F(x)} \tag{2}$$

where T is the return period; E is the drought inter-arrival time; and $F(x)$ is the marginal distribution function.

The multivariate joint return period can be divided into joint return period and conditional return period. Joint return period includes 'or' joint return period and 'and' joint return period. An 'or' return period means that at least one variable is greater than or equal to the given value. An 'and' return period indicates that all variables are greater than or equal to the given value. Due to the differences between 'or' and 'and' issues are theoretically expected and well known, this study focusses on the study of 'and' return period. The bivariate 'and' joint return periods can be defined as follows.

$$T_{\text{and}} = \frac{E}{1 - F(x_1) - F(x_2) + C(x_1, x_2)} \tag{3}$$

The trivariate joint return period is similar with the bivariate situation.

$$T_{\text{and}} = \frac{E}{1 - F(x_1) - F(x_2) - F(x_3) + C(x_1, x_2) + C(x_1, x_3) + C(x_2, x_3) - C(x_1, x_2, x_3)} \tag{4}$$

In the practical application, it is usual to evaluate the variable values for a fixed return period. However, it can be seen from Eqs. 3 to 4 that there are infinite pairs of variable values for a specific multivariate return period. To avoid this issue, we calculated the return period of fixed drought variables.

4 Results and discussion

4.1 Characteristic of drought variables

Using run theory, 64,448 drought events were extracted during 1961–2013. On average, there are about 79.6 drought events per site. Drought variables of all drought events, including duration, severity and peak, have been recorded. More details can be found in previous paper (Liu et al. 2015). In order to fit the marginal distribution better, the boxplot of drought variables is given out in Fig. 3. It can be seen that the distribution of duration, severity and peak all showed tail behavior. Therefore, it is necessary to select suitable marginal functions that can represent the tail characteristic.

Kendall's tau coefficient was used to test whether the variables are independent in time. The average Kendall value is 0.058, −0.065, −0.076 for D, S, P, respectively. There are 740, 745,733 stations' absolute value is less than 0.2 for D, S, P, respectively. Therefore, all variables (P–S–D) can be treated as independent in time.

According to SPEI classification, when the drought peak is bigger than 2, the drought event is considered as extreme drought, which accounts for about 5 % of all drought events. The relative drought duration is about 6 months, and the relative drought severity is about 9. So the scenario ($D \geq 6$, $S \geq 9$, $P \geq 2$) was selected as extreme drought variable.

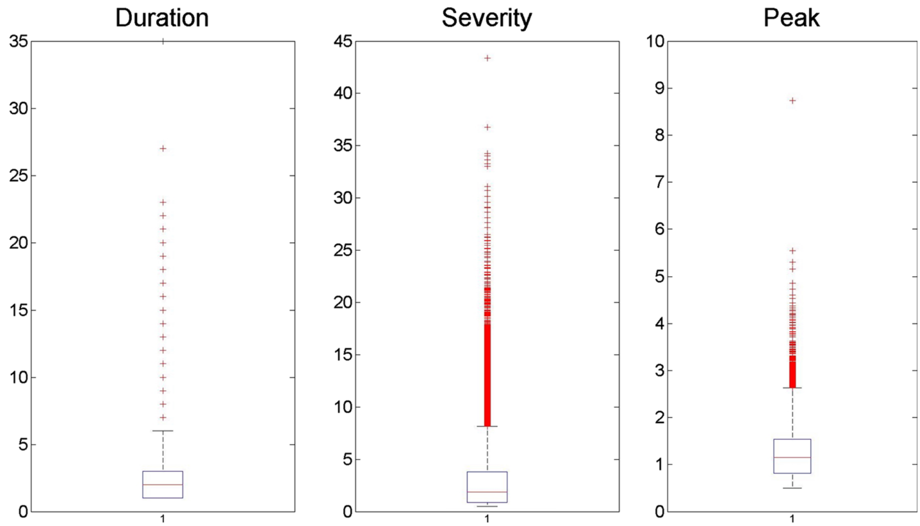

Fig. 3 *Boxplot* of drought variables

4.2 Univariate marginal distribution

Drought duration, severity and peak were fitted by the aforementioned marginal distributions. Note that discrete drought duration was treated as continuous data. The parameters of all distribution functions were estimated by MLE. The AIC was calculated for all sites. Limited by the length of this article, the parameters and AIC of the six marginal distributions would not be listed. The best marginal distribution of duration, severity and peak is shown in Fig. 4.

From Fig. 4a, it can be seen that the best marginal distribution of duration is exponential distribution. Gaussian distribution is the best marginal distribution only in two sites, and there is no optimal site for the other four marginal distributions. Therefore, exponential distribution was used to fit drought duration in the whole country.

Figure 4b shows the best marginal distribution of drought severity. There is no Gaussian distribution, and only five sites' best marginal is GEV. The count of other four marginal distributions is similar, but the spatial distribution has certain differences. Exponential distribution has a certain aggregation in the lower reaches of the Yangtze River and Guangxi Province. Weibull distribution has aggregation in Yunnan. GDP performs much better in the northern China, especially in the northeast China and southern Xinjiang. Gamma distribution is relatively uniform in China. For the huge number of sites used in this paper, we would like to choose a unified approach for whole country to reduce the complexity. At last, Weibull distribution was selected for its average AIC of all sites is the smallest.

It can be seen from Fig. 4c that GDP is the best marginal distribution in whole China. GEV and Weibull distribution is also the best marginal distribution in a certain amount of sites. GEV has aggregation in the southern Xinjiang. The distribution of Weibull distribution in China is relatively uniform. At last, GDP was selected to fit the marginal distribution of drought peak in the whole China.

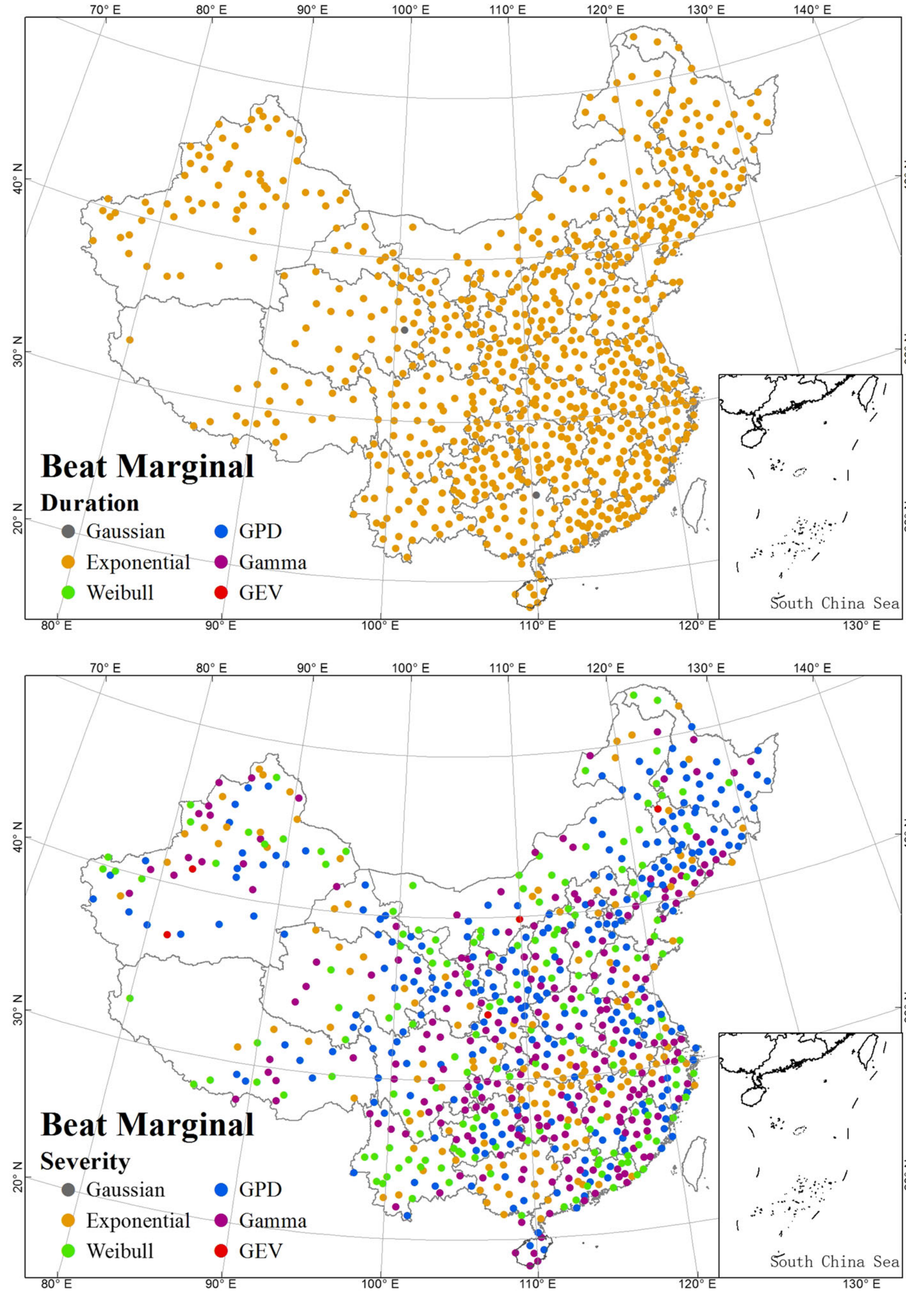

Fig. 4 Best marginal distribution of three drought variables

Zhang et al. found that GEV is the best marginal distribution for duration and severity in Yunnan based on CI index (Zhang et al. 2015). Similar with Shiau, Liu used exponential distribution to fit drought duration, and Gamma distribution to fit severity for SPI-based

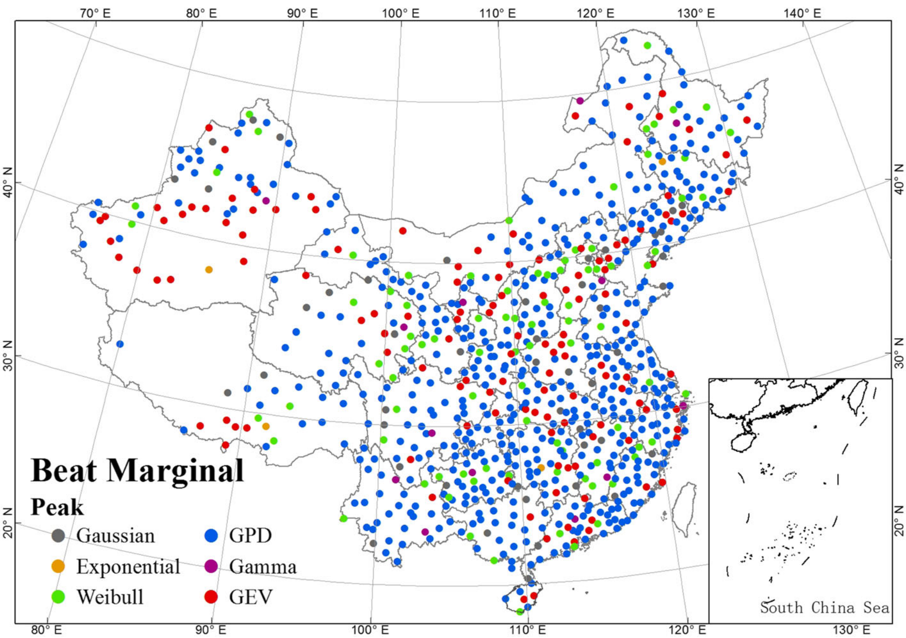

Fig. 4 continued

droughts. It can be seen that the conclusion of Shiau and Liu is similar with this article, while the conclusion of Zhang is different from this article. This is for the calculation method of SPEI is similar to SPI. Therefore, the choice of marginal distribution is affected by the nature of data.

4.3 Multivariate joint distribution

The correlations between drought characteristics were tested using the Kendall's tau coefficient. The average results across all sites are shown in Fig. 5. The correlation between D–P is poor, while the correlation between D–S, S–P is much higher. These results indicate that significant correlations between drought variables show that these variables should be modeled jointly.

The spatial distribution is not the same of the three correlations. The correlation of D–S is much higher in southeast China and Xinjiang Province, while it is relatively low in northeast China, Shaanxi and Shanxi. The correlation of D–P is good in southern China, but relatively poor in northern China, Jiangxi and Guangdong. The correlation of S–P is poor in Henan, Xinjiang, south part of northeast and the border between Hubei and Hunan.

Five commonly used Copula functions (including Gaussian, T, Frank, Clayton and GH Copula) were selected as candidates for the joint distribution (D–S, D–P, S–P and D–S–P). The nested Archimedean Copula was used to construct the trivariate joint distribution. The parameters of all Copulas were estimated using MLE. The best Copula for all sites is shown in Fig. 6.

The best Copula for D–S and D–P is GH Copula. The count of GH Copula is 593 and 526, respectively. There are few other Copulas with no significant aggregation. The poorest

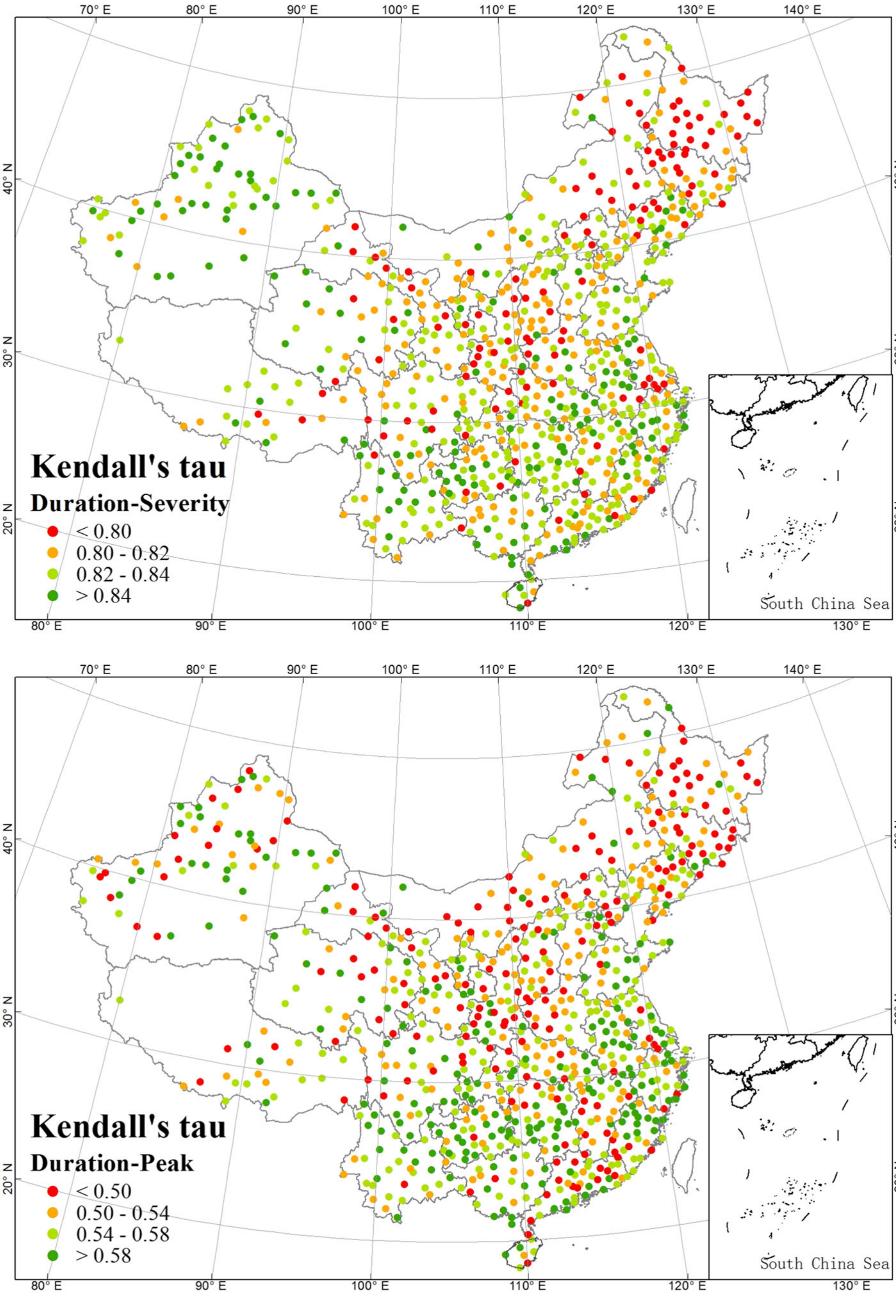

Fig. 5 Spatial distribution of Kendall's tau coefficient

Copula is Frank Copula. The best Copula for S–P is Frank Copula. There are few other Copulas. Only Clayton Copula has aggregation in southern Xinjiang. For trivariate, Gaussian, Clayton and GH copula all get acceptable results. T Copula and Frank Copula

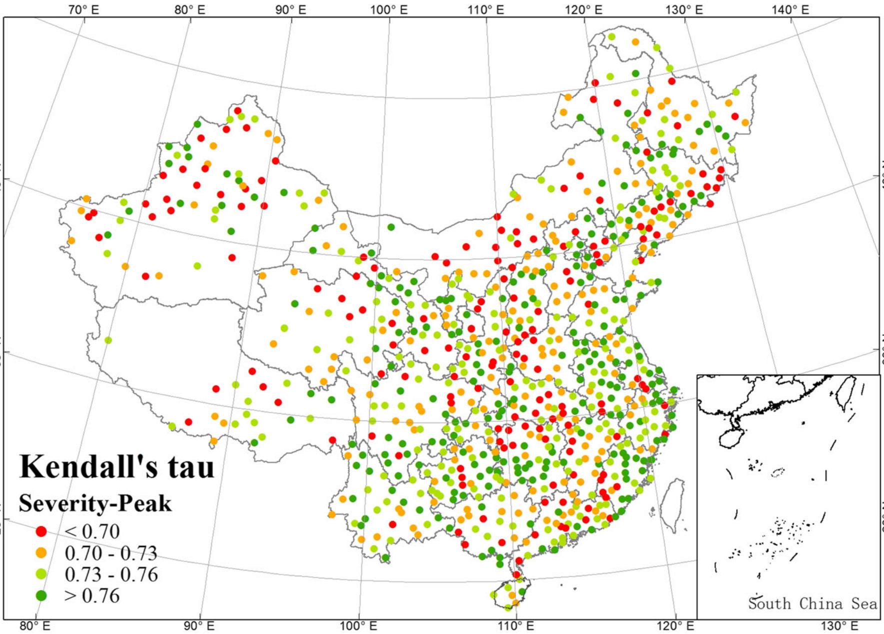

Fig. 5 continued

are much few. Gaussian mainly distributes in the southern part of northeast China, the lower reaches of Yangtze River, Guangxi and northern Xinjiang. The average AIC of Gaussian Copula is the smallest. Clayton Copula has aggregation in southern Xinjiang, but there are few in central China, Guangxi and Inner Mongolia. There are few stations' best Copula is GH Copula in the lower reaches of Yangtze River, Yunnan–Guizhou Plateau, Guangxi and Xinjiang. For simplicity, Gaussian Copula was chosen to fit the trivariate joint distribution.

4.4 Spatial distribution of univariate return period

Using Eq. 2, the univariate return period of duration, severity and peak was calculated. The results were interpolated to raster to cover the whole area of China using inverse distance weighted (IDW). To distinguish the short return period and long return period, two contours were added. Only those patches with large areas were kept. The results are shown in Fig. 7.

Figure 7a shows the spatial distribution of the return period corresponding to duration longer than or equal to 6 months. The return period varies from 4.4 to 22.1 years, and has an average of 9.2 years. Short return period areas are mainly concentrated in southern China and western China, especially in southern Hubei, northern Hunan, western Qinghai and northern Xinjiang. Long return period areas are mainly distributed in northeast China, central Shaanxi and the coastal regions of Fujian. These regions are likely to happen once every 12 years on average. Figure 7b shows the spatial distribution of the return period corresponding to a severity greater than or equal to 9. The return period varies from 7.3 to

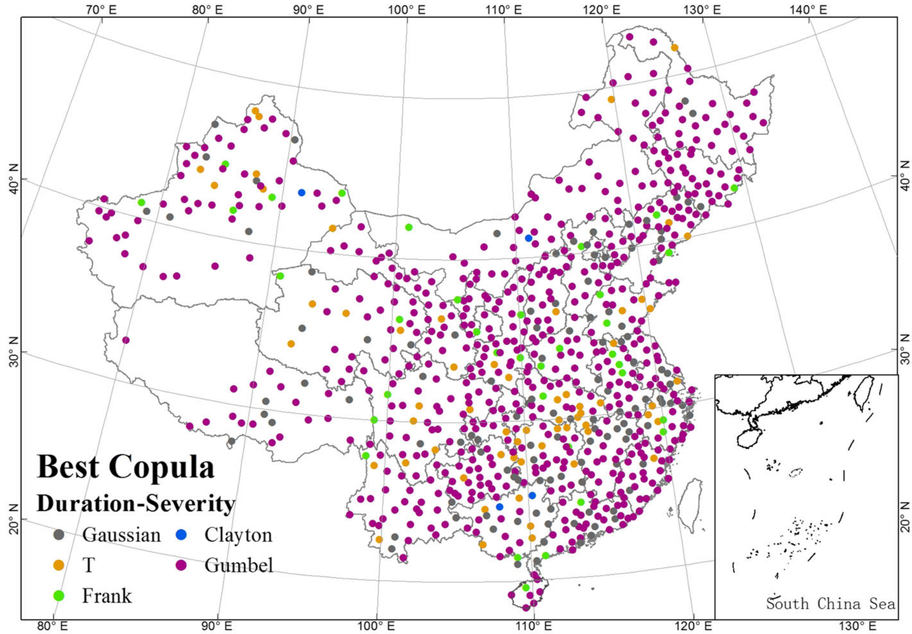

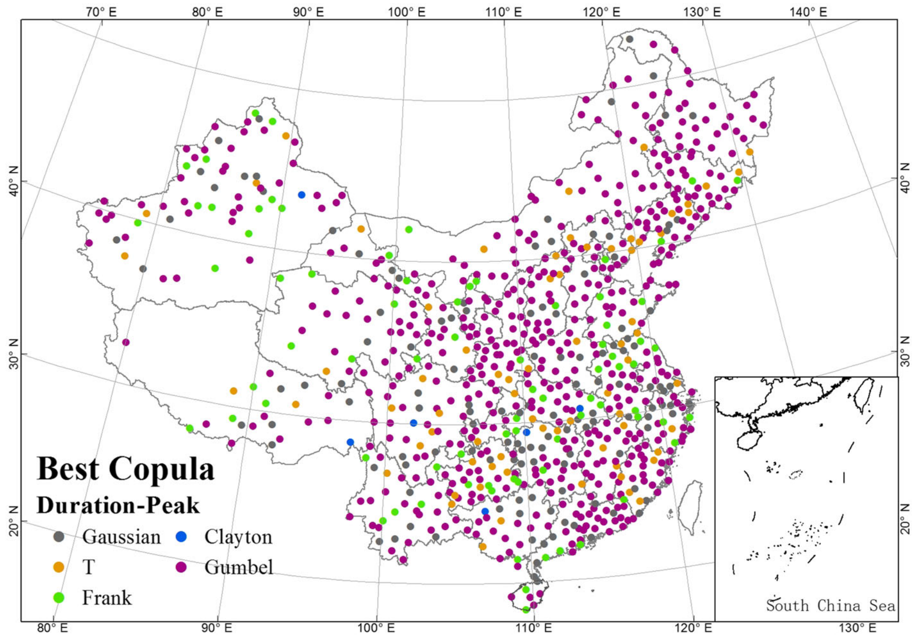

Fig. 6 Best Copula for D–S, D–P, S–P and D–S–P

36.5 years, and has an average of 15.9 years. Short return period areas are mainly distributed in northwest China, Yunnan–Guizhou Plateau, Zhejiang, northern Jiangxi and northern Anhui. Long return periods are distributed in northeast China, Shaanxi, Henan

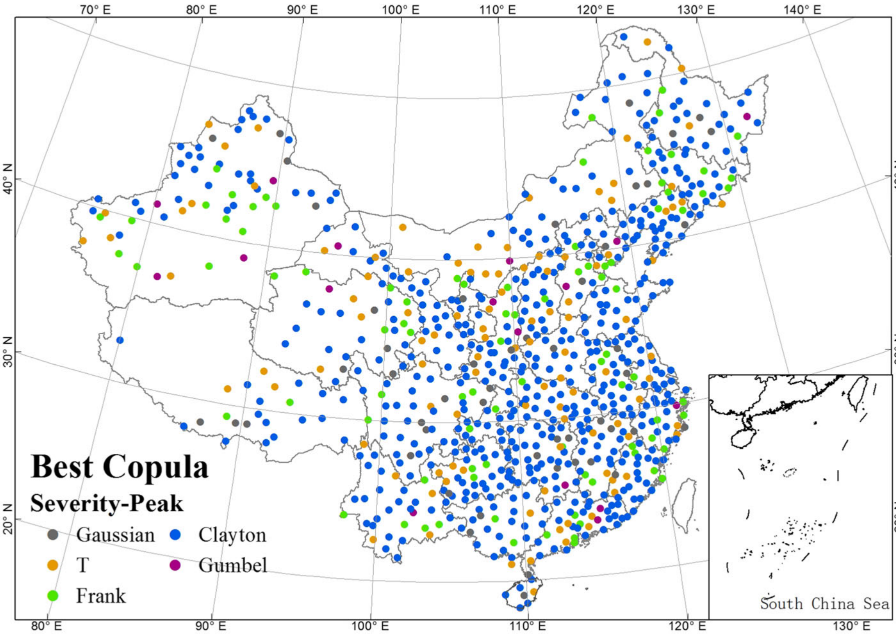

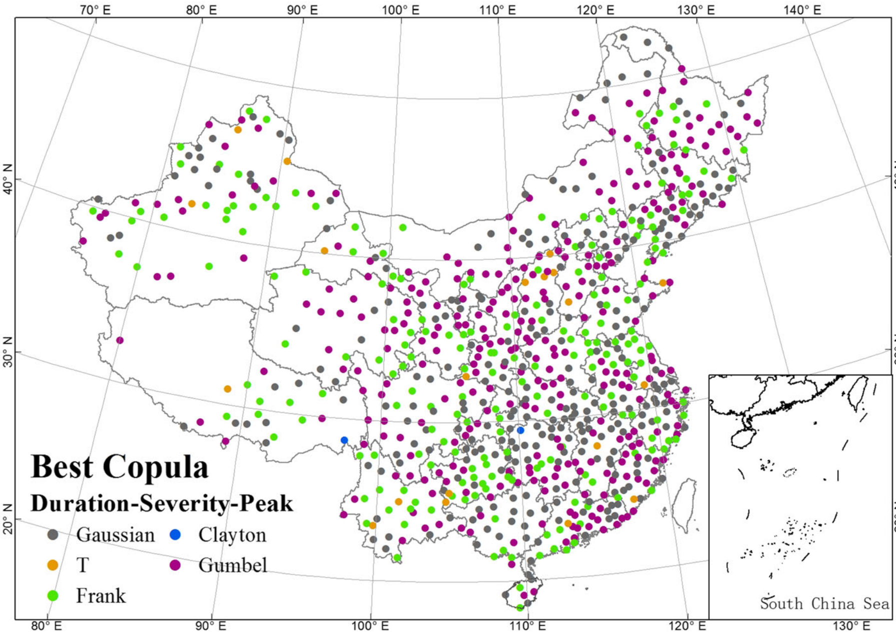

Fig. 6 continued

and northeast Qinghai. Figure 6c shows the spatial distribution of the return periods corresponding to a peak greater than or equal to 2. The return period of the peak values varies from 5.0 to 45.73 years, with an average of 14.2 years. Short return period areas are located in eastern China, with a period of approximately 10 years. The return period is

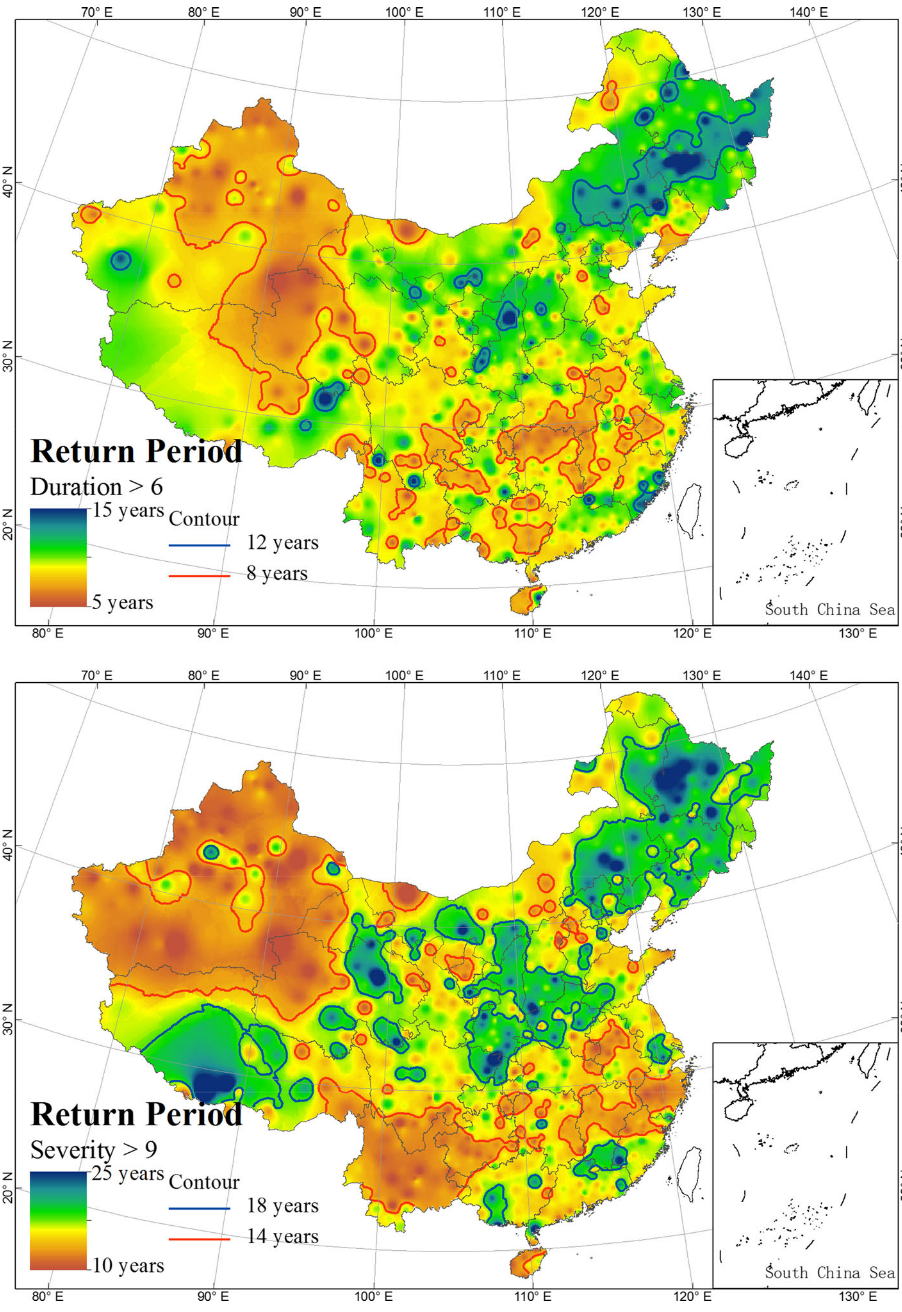

Fig. 7 Spatial distribution of univariate return period: **a** D; **b** S; **c** P

especially short in the lower reaches of the Yangtze River, Guangdong, Guangxi and western Hunan, while the return period is much longer in western China, with the exception of northern Xinjiang.

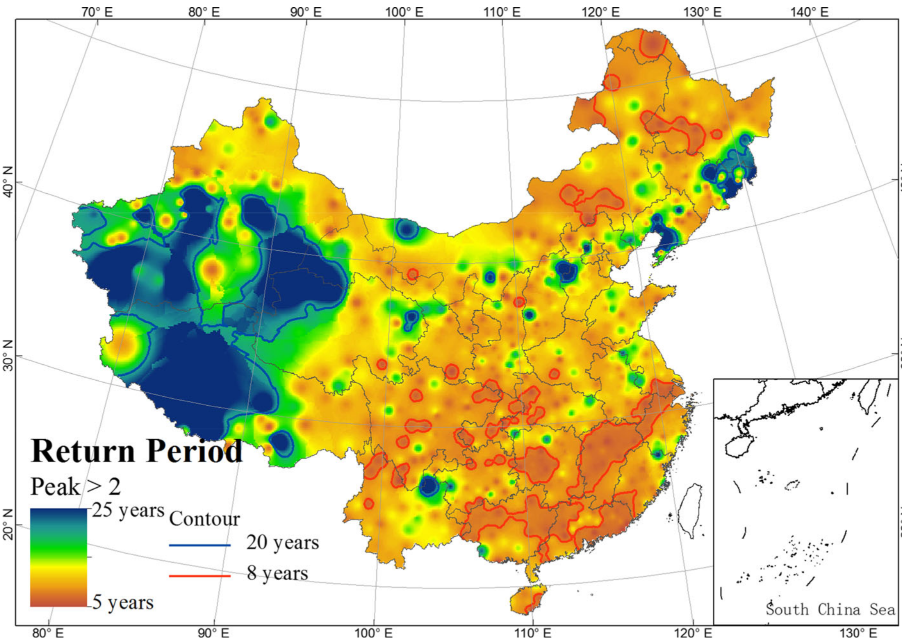

Fig. 7 continued

Therefore, it can be concluded that the univariate return period of the given value is approximately 10–15 years on average. The spatial distribution of drought characteristics indicates large differences, especially with respect to D–P and S–P. The return period of extreme droughts is much shorter in southern China. However, it should be noted that a single drought characteristic is insufficient to describe all drought events.

4.5 Spatial distribution of bivariate return period

Equation 3 was used to calculate the bivariate joint return period. Similar to the univariate return period, the bivariate return periods are also interpolated to raster using IDW, and are shown in Fig. 8.

The return period of D and S varies from 7.4 to 37 years, and has an average of 16.8 years. Short return periods are mainly distributed in northwest China, the Yunnan–Guizhou Plateau and the middle and lower reaches of the Yangtze River. The return period is also short in eastern Shandong, central Hebei and the coastal area of Guangzhou, with an average return period of less than 15 years, while northeast China, Shaanxi and southern Shanxi have a longer return period of greater than 20 years. The return period of D and P varies from 8.4 to 40.3 years, with an average of 24.1 years. Short return periods are mainly distributed in the northern Jiangxi, the central Hunan and the border between Zhejiang and Yunnan. The return period of S and P varies from 11.1 to 66.0 years, with an average of 31.2 years. The return period is short at the border between Zhejiang and Jiangxi, the west part of Hunan, the border between Yunnan, Sichuan, and Guizhou and the coastal area of Guangdong.

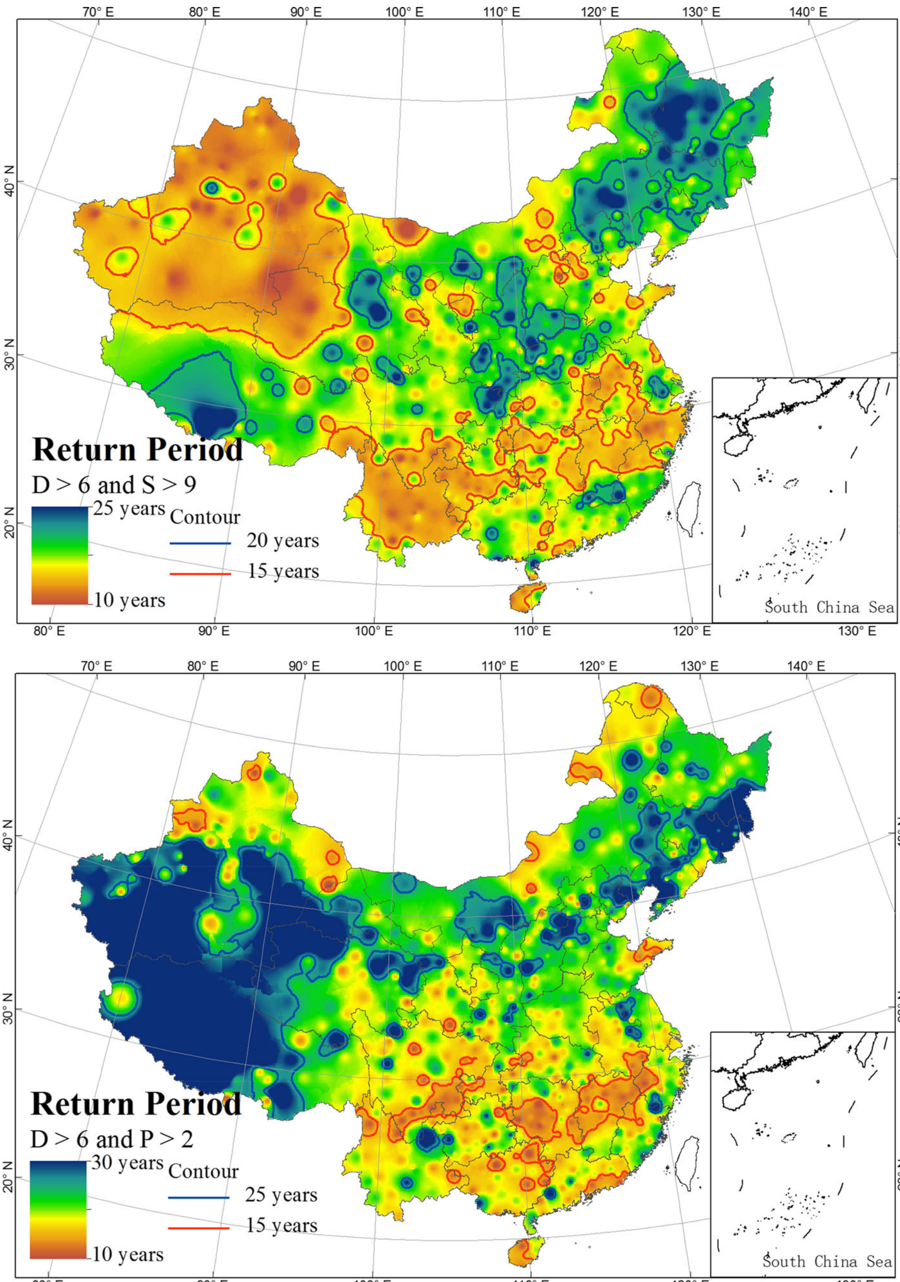

Fig. 8 Spatial distribution of bivariate return periods: **a** D and S; **b** D and P; **c** S and P

The return period is more than 20 years, which is much longer than univariate return period. Many researchers have studied the drought return period in China based on bivariate joint distribution (Liu et al. 2011; Zhang et al. 2012, 2015). Due to differences in

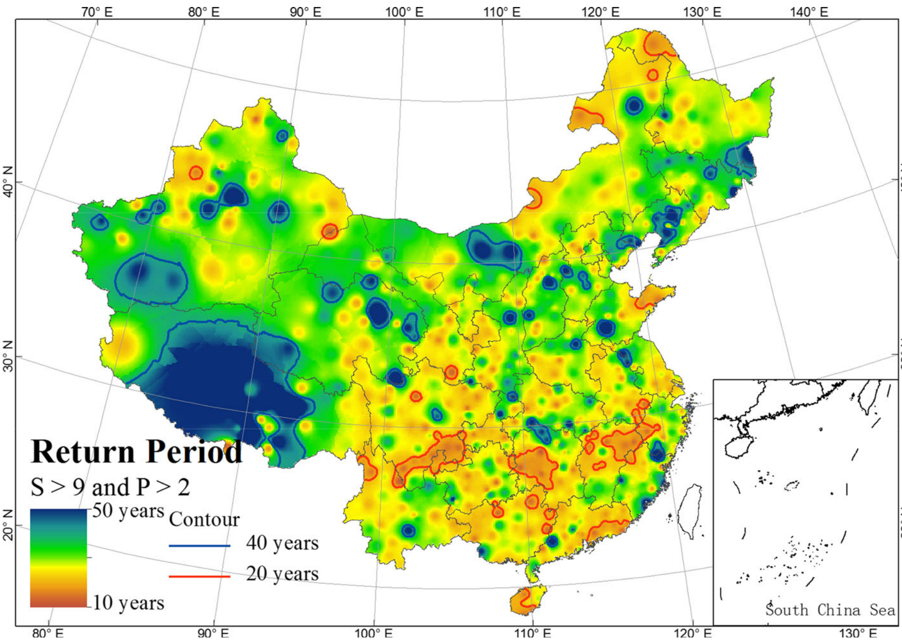

Fig. 8 continued

research data and method, numerical differences exist between this paper and previous researches undertaken; however, the spatial distribution is consistent.

4.6 Spatial distribution of trivariate return period

Equation 4 was used to calculate the trivariate joint return period. The interpolated trivariate joint return period is shown in Fig. 8.

Figure 9 indicates the trivariate return period varies from 14.5 to 93.5 years, with an average of 42.1 years. The short return period is mainly distributed in southern China, including the border between Sichuan and Yunnan, the coast area of Guangdong, western Hunan and northern Jiangxi.

These results indicate that trivariate return period is much longer than bivariate return period. For each station, extreme droughts may occur once every 40 years. Extreme droughts are most likely to occur in the middle and lower reaches of the Yangtze River, southwest China and the coastal area of Guangdong. These areas are economically developed with large populations; thus, extreme drought events place severe threats to the security of water resources in these regions. For example, from October to April 2010, an extreme drought event struck southwest China. The cumulative rainfall was less than 100 mm over seven consecutive months in Kunming, Chuxiong, Qujing and surrounds. At Chuxiong Station, the drought event began in September 2009 and continued until September 2010. This drought event lasted 13 months with a 19.5 severity ranking and a peak of 1.93, with the trivariate return period of this drought event reaching 400 years.

The formation of the extreme drought can be attributed to anomalies in the large-scale atmospheric circulation. The annual precipitation is high in southern China, but it is not

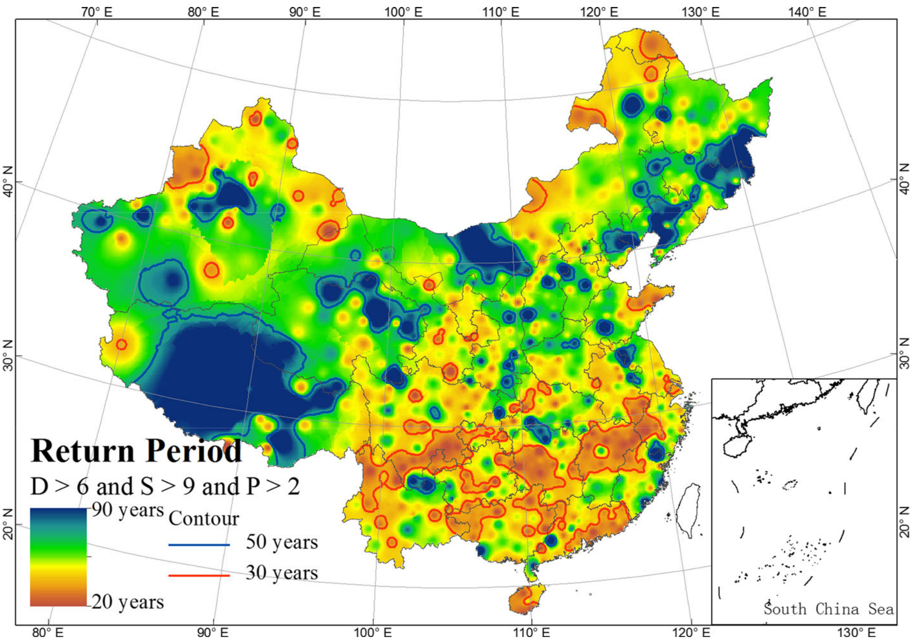

Fig. 9 Spatial distribution of trivariate return period

evenly distributed over the seasons. For example, the coastal areas of Guangdong are prone to drought in spring as a result of less frontal precipitation and strong evaporation (Zhang et al. 2010). The local terrain also plays an important role, with the Foehn effect and topographical enclosure leading to less precipitation and hotter climates. This was observed more markedly in Hengyang and Shaoyang of Hunan Province and northern Yunnan. Local landforms and geology may also contribute to drought conditions, with areas of poor water-holding capacity, such as karsts, increasing the local effects of droughts.

5 Conclusion

As drought is a critical climate disaster, understanding the characteristics of droughts is an essential step to construct efficient mitigation measures for drought-related problems. In this study, drought was identified through the calculation of 810 individual SPEI series and the utilization of run theory. A drought event is described by three variables: duration, severity and peak. These variables are separately modeled by different marginal distributions. As the dependence assessment indicated a high dependence between these variables, Copula functions were found effective in linking the fitted model and the construction of the joint distribution function. Based on the return period function, the univariate, bivariate and trivariate return periods were calculated and the corresponding spatial distributions were discussed.

Six commonly used marginal distributions were investigated, which identified that Exponential function, Weibull function and Pareto function provide the best goodness of fit for duration, severity and peak, respectively. Five Copula functions were employed to construct the bivariate and trivariate joint probability distribution. The GH Copula was effective in calculating the joint distribution of D–S and D–P. Clayton Copula and Gaussian are suit to construct the joint distribution of S–P and D–S–P. The spatial distribution of best marginal and best Copula shows that the fitting effect of others functions may be better for some special regions.

The spatial distributions of different return periods also have highlighted significant differences. The trivariate return period varies from 4.7 to 27.2 years under extreme drought conditions. The short return period is mainly distributed in southern China, including the border between Sichuan and Yunnan, the coast area of Guangdong, western Hunan and northern Jiangxi. This is significant for identifying methods of drought control and resistance, and can provide effective support for drought assessment.

Acknowledgments The authors wish to thank the editor. The data were obtained from China Meteorological Data Sharing Service System. This work was supported by the National Natural Science Foundation of China (Grant Nos. 41201441, 41301501 and 41371363).

Compliance with ethical standards

Conflict of interest The authors declare that they have no conflict of interests.

References

Akaike H (1974) A new look at the statistical model identification. Autom Control 19:716–723

Andreadis KM, Lettenmaier DP (2006) Trends in 20th century drought over the continental United States. Geophys Res Lett 33:L10403

Atkinson PM, Lloyd CD (1998) Mapping precipitation in Switzerland with ordinary and indicator kriging. J Geogr Inf Decis Anal 2:72–86

Bonaccorso B, Cancelliere A, Rossi G (2003) An analytical formulation of return period of drought severity. Stoch Environ Res Risk Assess 17:157–174

da Costa Dias A (2004) Copula inference for finance and insurance. Diss., Mathematische Wissenschaften, Eidgenössische Technische Hochschule ETH Zürich, Nr. 15283, 2004

Favre AC, El Adlouni S, Perreault L, Thiémonge N, Bobée B (2004) Multivariate hydrological frequency analysis using Copulas. Water Resour Res 40:290–294

Gocic M, Trajkovic S (2014) Spatiotemporal characteristics of drought in Serbia. J Hydrol 510:110–123

González J, Valdés JB (2003) Bivariate drought recurrence analysis using tree ring reconstructions. J Hydrol Eng 8:247–258

Gräler B, van den Berg M, Vandenberghe S, Petroselli A, Grimaldi S, Baets BD, Verhoest N (2013) Multivariate return periods in hydrology: a critical and practical review focusing on synthetic design hydrograph estimation. Hydrol Earth Syst Sci 17:1281–1296

Grimaldi S, Serinaldi F (2006) Asymmetric Copula in multivariate flood frequency analysis. Adv Water Resour 29:1155–1167

Hernandez EA, Uddameri V (2014) Standardized Precipitation Evaporation Index (SPEI)-based drought assessment in semi-arid south Texas. Environ Earth Sci 71:2491–2501

Janga RM, Ganguli P (2012) Application of Copulas for derivation of drought severity–duration–frequency curves. Hydrol Process 26:1672–1685

Joe H (1997) Multivariate models and multivariate dependence concepts. Chapman & Hall, London

Kim TW, Valdés JB, Yoo C (2003) Nonparametric approach for estimating return periods of droughts in arid regions. J Hydrol Eng 8:237–246

Kim TW, Valdés JB, Yoo C (2006) Nonparametric approach for bivariate drought characterization using Palmer Drought Index. J Hydrol Eng 11:134–143

Liu C-L, Zhang Q, Singh VP, Cui Y (2011) Copula-based evaluations of drought variations in Guangdong, South China. Nat Hazards 59:1533–1546

Liu X, Wang S, Zhou Y, Wang F, Li W, Liu W (2015) Regionalization and spatiotemporal variation of drought in China Based on Standardized Precipitation Evapotranspiration Index (1961–2013). Adv Meteorol 2015:950262. doi:10.1155/2015/950262

Lorenzo-Lacruz J, Vicente-Serrano SM, López-Moreno JI, Beguería S, García-Ruiz JM, Cuadrat JM (2010) The impact of droughts and water management on various hydrological systems in the headwaters of the Tagus River (central Spain). J Hydrol 386:13–26
Lu E, Luo Y, Zhang R, Wu Q, Liu L (2011) Regional atmospheric anomalies responsible for the 2009–2010 severe drought in China. J Geophys Res Atmos 116:1471–1479
Lu J, Ju J, Ren J, Gan W (2012) The influence of the Madden-Julian Oscillation activity anomalies on Yunnan's extreme drought of 2009–2010. Sci China Earth Sci 55:98–112
Michele C, Salvadori G, Vezzoli R, Pecora S (2013) Multivariate assessment of droughts: frequency analysis and dynamic return period. Water Resour Res 49:6985–6994
Mirabbasi R, Fakheri-Fard A, Dinpashoh Y (2012) Bivariate drought frequency analysis using the copula method. Theor Appl Climatol 108:191–206
Mirakbari M, Ganji A, Fallah S (2010) Regional bivariate frequency analysis of meteorological droughts. J Hydrol Eng 15:985–1000
Mishra AK, Desai VR (2005) Spatial and temporal drought analysis in the Kansabati river basin, India. Int J River Basin Manag 3:31–41
Mishra AK, Singh VP (2010) A review of drought concepts. J Hydrol 391:202–216
Nelsen RB (1999) An introduction to Copulas. Springer, New York
Qiu H, Cao M, Hao J, Wang Y, Wang Y (2013) Relationship between frequency and magnitude of drought damage in China in 1950–2010. Sci Geogr Sin 33:576–580 **(in Chinese)**
Serinaldi F, Bonaccorso B, Cancelliere A, Grimaldi S (2009) Probabilistic characterization of drought properties through Copulas. Phys Chem Earth 34:596–605
Shiau JT (2006) Fitting drought duration and severity with two-dimensional Copulas. Water Resour Manag 20:795–815
Shiau JT, Modarres R (2009) Copula-based drought severity–duration–frequency analysis in Iran. Meteorol Appl 16:481–489
Sklar M (1959) Fonctions de répartition à n dimensions et leurs marges. Publ Inst Stat Univ Paris 8:229–231
Song S, Singh VP (2010) Meta-elliptical Copulas for drought frequency analysis of periodic hydrologic data. Stoch Environ Res Risk Assess 24:425–444
Song S, Cai H, Jin J, Kang Y (2012) Copulas function and its application in hydrology. Science Press, Beijing **(in Chinese)**
State Flood Control and Drought Relief Office, the Ministry of Water Resources of the People's Republic of China (2011) Bulletin of flood and drought disasters in China. China Water Power Press, Beijing **(in Chinese)**
Thornthwaite CW (1948) An approach toward a rational classification of climate. Geogr Rev 38:55–94
Vicente-Serrano SM (2006) Spatial and temporal analysis of droughts in the Iberian Peninsula (1910–2000). Hydrolog Sci J 51:83–97
Vicente-Serrano SM, Beguería S, López-Moreno JI (2010a) A Multiscalar Drought Index sensitive to global warming: the Standardized Precipitation Evapotranspiration Index. J Climate 23:1696–1718
Vicente-Serrano SM, Beguería S, López-Moreno JI, Angulo M, El Kenawy A (2010b) A new global 0.5 gridded dataset (1901–2006) of a Multiscalar Drought Index: comparison with current Drought Index datasets based on the Palmer Drought Severity Index. J Hydrometeorol 11:1033–1043
Wang Q, Wu J, Lei T et al (2014) Temporal-spatial characteristics of severe drought events and their impact on agriculture on a global scale. Quatern Int 349:10–21
Wilhite DA (2000) Drought as a natural hazard: concepts and definitions. Drought Glob Assess 1:3–18
Wilhite DA, Glantz MH (1985) Understanding: the drought phenomenon: the role of definitions. Water Int 10:111–120
Wong G, Lambert MF, Leonard M, Metcalfe AV (2009) Drought analysis using trivariate Copulas conditional on climatic states. J Hydrol Eng 15:129–141
Xiao M, Zhang Q, Chen X (2012) Spatial-temporal patterns of drought risk across the Pearl River Basin. Acta Geogr Sin 67:83–92 **(in Chinese)**
Yevjevich V, Ingenieur J (1967) An objective approach to definitions and investigations of continental hydrologic droughts. Water Resour Publ, Fort Collins
Zhang Z (2009) Milestones of drought mitigation work in China—understanding of "People' Republic of China drought resistance ordinance". China Water Resour 6:19–21 **(in Chinese)**
Zhang Q, Jiang T, Chen YD, Chen X (2010) Changing properties of hydrological extremes in south China: Natural variations or human influences? Hydrol Process 24:1421–1432
Zhang Q, Xiao M, Singh VP, Li J (2012) Regionalization and spatial changing properties of droughts across the Pearl River basin, China. J Hydrol 472:355–366
Zhang D, Yan D, Lu F, Wang Y, Feng J (2015) Copula-based risk assessment of drought in Yunnan province, China. Nat Hazards 75:2199–2220